Geophysical Journal International

Geophys. J. Int. (2011) doi: 10.1111/j.1365-246X.2011.05077.x

Comparing extension on multiple time and depth scales in the Corinth Rift, Central Greece

Rebecca E. Bell,* Lisa C. McNeill, Timothy J. Henstock and Jonathan M. Bull

*School of Ocean and Earth Science, University of Southampton, National Oceanography Centre, Southampton, SO*14 3*ZH, UK.*
E-mail: rebecca.bell@imperial.ac.uk

Accepted 2011 May 10. Received 2011 May 5; in original form 2011 January 17

SUMMARY

The young (< 5 Ma) Corinth Rift is an ideal natural laboratory to investigate rift deformation mechanisms by comparing extension rates determined by various methods spanning different depth and time ranges. Corinth Rift geodetic extension rates averaged over 5–100 yr have been interpreted to increase from ∼5 mm yr^{-1} or less in the east to >10–15 mm yr^{-1} in the west. We quantify total upper-crust and whole-crust extension on three profiles across the Corinth Rift. Whole-crust extension is greater across the central rift (∼11–21 km) than across the western part of the rift (∼5–13 km). This correlates with the overall rift morphology, which shows maximum basement subsidence, sediment accumulation, rift width and greatest summed Late Quaternary fault displacements in the central basin, but contrasts with the pattern of geodetic extension rates which are greater to the west of the central basin. The E–W increase in strain rates interpreted from geodetic data cannot have persisted over rift history to produce the observed rift morphology. We suggest the discrepancy between short-term and long-term extension patterns is related to shifts in the loci of maximum extension due to fault growth and linkage during Corinth Rift history, and is likely a characteristic of rift development in general. Total upper-crust and whole-crust extension estimates in the western rift, where extension estimates are best constrained, are within error. We propose that uniform pure-shear extension is a viable extension mechanism in the western rift and crustal extension estimates do not require the existence of a major active N–S dipping detachment fault.

Key words: Continental tectonics: extensional; Sedimentary basin processes; Neotectonics; Fractures and faults; Europe.

INTRODUCTION

Methods to determine extension across a rift zone are sensitive to different depth intervals and time periods. Cumulative fault offset across a rift zone provides an estimate of upper-crust extension, while crustal thinning and basement subsidence indicate whole-crust extension. Recent and Late Quaternary extension rates can be assessed from Global Positioning System (GPS) techniques and fault activity. Comparisons and discrepancies between extension over different depth and timescales can reveal extension mechanisms and strain patterns during rifting.

GPS is often used to investigate crustal deformation on a decadal timescale, and to constrain models of longer term tectonics (e.g. Wallace *et al.* 2009). However, in some cases, patterns of GPS-derived crustal deformation differ from patterns inferred from geology, geomorphology or historical seismicity (e.g. Dixon *et al*. 2003). These discrepancies may imply rapidly varying deformation, variations in strain over the seismic cycle or errors/bias in data or analysis (Dixon *et al*. 2003).

Some rifted continental margins show different degrees of extension in the upper crust and whole crust, suggesting depth-dependent extension (e.g. Kusznir *et al*. 2005), although others have argued that this is an artefact of incomplete data (e.g. Reston 2007). In contrast, mildly extended intracontinental rifts tend to have equal upper-crust and whole-crust extension implying that initial rifting may occur by largely uniform pure-shear thinning of the continental lithosphere (e.g. the North Sea, White 1990). The importance of high- versus low-angle normal fault activity in generating young rift systems has also been discussed at several young rift zones (Sorel 2000, e.g. Papua New Guinea and the Gulf of Corinth; Abers 2009), suggesting that simple-shear detachment faulting may be important in the early evolution of some rifts.

*Now at: Imperial College London, Exhibition Road, London SW7 2AZ, UK.

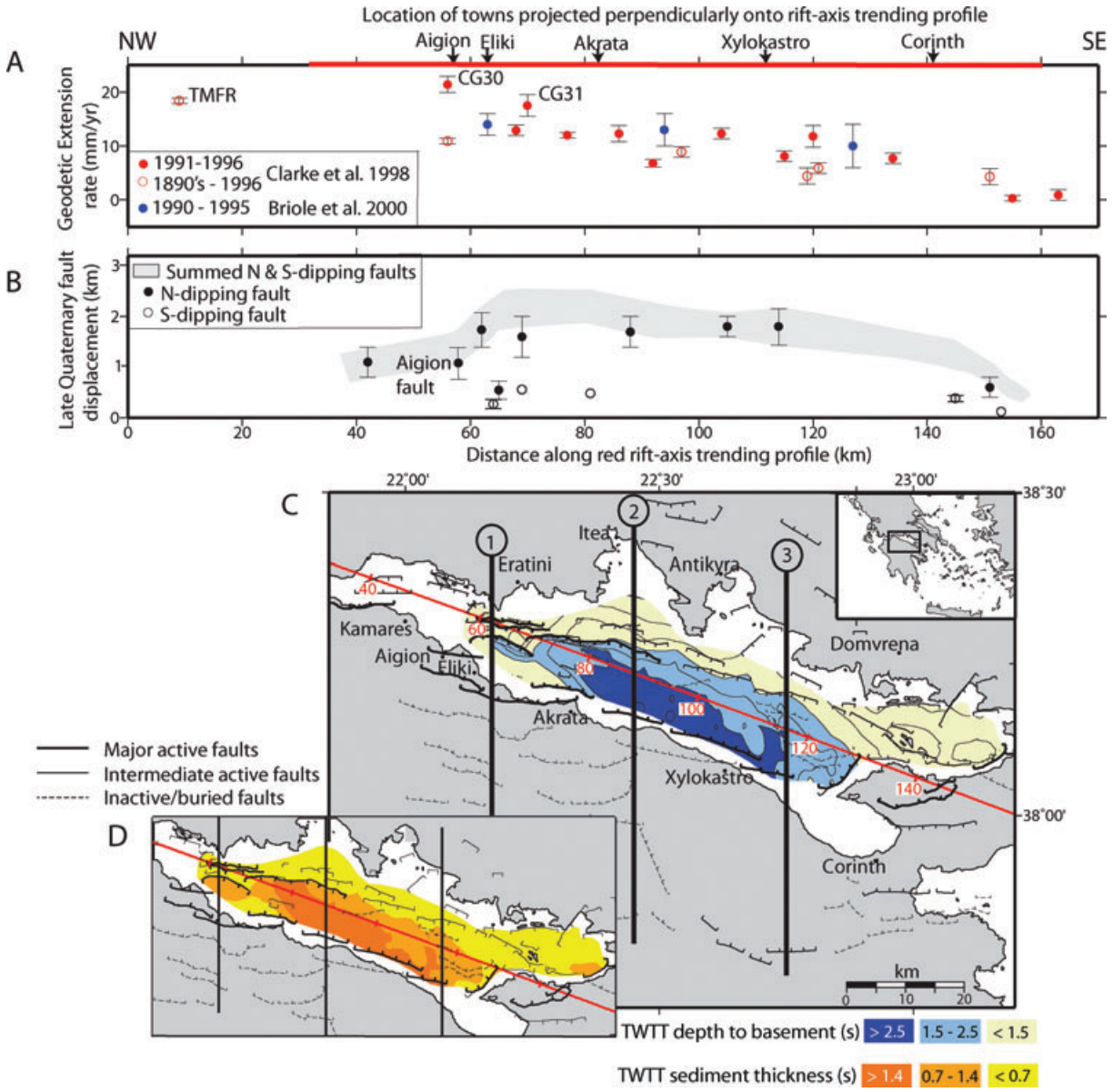

Figure 1. (A) Representative geodetic 'horizontal extension rates' across the Corinth Rift (Briole *et al.* 2000, blue circles; Clarke *et al.* 1998, red circles are estimates for the period 1991–1996, and white circles 1890s–1996). The red line indicates the extent of the profile shown in Fig.1(C). TMFR, CG30 and CG31 are site names from Clarke *et al.* (1998). (B) Summary of Late Quaternary fault displacement over the last ∼0.4 Myr for individual N- (black circles) and S-dipping (white circles) faults, derived from fault slip rates provided in Bell *et al*. (2009), fig. 13 and table 5. The Aigion fault is taken as initiating 0.3 Ma, where as all the other known faults existed pre-0.4 Ma (after Bell *et al.* 2009). The grey envelope is derived by summing Late Quaternary displacements for both N- and S-dipping faults across the rift and joining up data points to show the general trend of total Late Quaternary fault displacement along the rift. This envelope does not include contributions from unidentified faulting and details in the displacement profile along faults, which are currently unknown. (C) Transects 1–3 considered in this study (black lines) and basement depth for the offshore Corinth Rift (Bell *et al.* 2009). Fault interpretations follow Bell *et al.* (2009) and references therein. Red line shows the line of projection of GPS extension rates in Fig. 1(A), and the red numbers are distance along this profile in km. (D) Sediment thickness within the Gulf of Corinth after Bell *et al.* (2009).

The intracontinental Corinth Rift is seismically active, has a syn-rift infill uncomplicated by tectonic overprinting and is a key player in larger scale Aegean tectonics. The region has been undergoing N–S extension, against the N–S structural grain of the Pindos mountain chain since the Pliocene (e.g. Skourlis & Doutsos 2003). The currently active part of the Corinth Rift system initiated ∼1–2 Ma (e.g. McNeill *et al*. 2005; Leeder *et al*. 2008) with both terrestrial and marine components. In this paper the term 'Corinth Rift' refers to the region spanning the offshore Gulf of Corinth and Gulf of Alkyonides, and the onshore areas affected by faulting (Fig. 1). The terms 'western', 'central' and 'eastern' Corinth Rift refer to parts of the rift west of ∼22°15′, between ∼22°15′–22° 45′ and east of ∼22°45′, respectively.

Both 5- to 10-yr GPS and 100-yr triangulation–GPS velocity estimates suggest N–S extension at <5 mm yr^{-1} in the east and >15 mm yr^{-1} in the west (e.g. Clarke *et al.* 1998; Billiris *et al.* 1991), although some studies have proposed a less dramatic E–W gradient (e.g. Briole *et al.* 2000; Avallone *et al*. 2004; Floyd *et al*. 2010, Fig. 1A). The greatest GPS-derived extension rates from numerous studies occur at the longitude of the Eliki–Aigion

region, at a distance of ∼55–60 km along the rift-axis trending red profile in Fig. 1(C). However, there is significant variability in the reported magnitude of extension rates in this area (Fig. 1; 20–23 mm yr^{-1}, Clarke *et al*. 1998; 12–16 mm yr^{-1}, Briole *et al*. 2000; ∼16 mm yr^{-1}, Avallone *et al*. 2004). A continued increase in geodetic extension rates has been projected west of Aigion by Clarke *et al.* (1998) based on movement of an 1890 triangulation site. Higher north margin GPS velocities (relative to a fixed Peloponnese) are observed in locations west of Aigion than to the east from fig. 4 of Avallone *et al*. (2004), suggesting extension rates do increase to the west.

Estimates of Late Quaternary fault displacement over the last ∼400 kyr can be determined along the Corinth Rift from fault slip rates (summarized by Bell *et al.* 2009 and Fig. 1B), however Holocene averaged estimates of fault displacement are incomplete in the central rift. Summed Late Quaternary fault displacement, across both offshore and coastal active N- and S-dipping faults (shaded envelope in Fig. 1B), is greatest in the central part of the Corinth Rift between 67 km and 115 km along the rift-axis trending red profile in Fig. 1(C) (∼1.2–2.4 km). The greatest levels of Late Quaternary extension coincide with where the offshore Corinth Rift basin is deepest, sediment accumulations thickest and Gulf of Corinth widest (Figs 1C and D). Summed Late Quaternary fault displacement decreases west of 67 km and east of 150 km along the rift-axis profile in Fig. 1(C), producing an overall bell-shaped pattern in fault displacement along the rift (Fig. 1B).

The interpreted E–W increase in geodetic extension rates over the last 5–100 yr (Fig. 1, Clarke *et al*. 1998) mismatches the pattern of summed Late Quaternary fault displacement and overall rift morphology, which suggests long-term extension is greatest in the central rift, and decreases to the east and west (Fig. 1). The discrepancy between short-term geodetic extension rates and longer term patterns of extension along the rift has not previously been quantified.

In this study we quantify total extension across the Corinth Rift since its initiation using three methods: (1) upper-crust extension from faulting; (2) whole-crust extension from crustal thinning and (3) whole-crust extension from basement subsidence. These estimates of the amount of total stretching throughout rift history are compared with short-term geodetic rates to assess their applicability as proxies for long-term basin evolution.

UPPER-CRUSTAL EXTENSION FROM FAULT DISPLACEMENT

We estimate upper-crustal extension by summing fault heave, assuming that all extension in the upper crust is taken up on planar faults that can be identified on seismic sections or in the field. Due to the difficulty of picking fault planes and hence determining fault dip on seismic sections, it is more accurate to measure the throw on a fault and determine heave for a range of fault dips (Lamarche *et al.* 2006).

Total extension has been estimated from the net throw on basement-offsetting faults along transects 1–3 (Fig. 1C), which are roughly perpendicular to the rift-axis. No profile was generated across the easternmost Corinth Rift due to the large uncertainty in the activity of onshore faults in this area. Active offshore and coastal faults and basement depth along these transects follow the interpretations of seismic reflection and compiled field observations from Bell *et al.* (2009) and references therein (Figs 1C & 2). Onshore, largely inactive, faults follow Collier & Jones (2003), Leeder *et al*. (1991), Roberts (1996), Rohais *et al.* (2007) and Ford *et al.* (2007) (Figs 1C & 2). We use different methods (described in the Supporting Information) to determine fault throw if the fault is (1) offshore, (2) partially offshore and onshore and (3) onshore. These three methods are increasingly poorly constrained (from 1 to 3), due to decreasing direct basement depth information and additional assumptions. However, they provide the current best estimate of total extension across Corinth Rift faults, using all data available. Throw and throw uncertainty estimates for each fault are shown in Fig. 2.

The best estimates of net throw for each fault have been summed, and converted to heave (i.e. extension) using a fault dip range of 40–60°, based on Corinth Rift fault planes exposed onshore (Collier & Jones 2003), earthquake focal mechanisms (Hatzfeld *et al*. 2000) and offshore seismic sections (Bell *et al*. 2008, Table 1). Some focal mechanism studies have suggested that in the western rift active faults dip at only 30° (Bernard *et al*. 1997), however we do not observe clear fault planes with these dip angles in available seismic profiles (Bell *et al*. 2008).

Our results show that summed net extension across the rift zone (faults shown in Table 1) is slightly greater along transects 1 and 2 (∼5–13 km) than along transect 3 (∼4–9 km). Total upper-crust extension estimates are best constrained along transect 1, where high-resolution seismic data exist offshore (Bell *et al*. 2008) and south coast faults are well documented in the literature. Along transects 2 and 3 further east, likely unknown south coast onshore faults mean our estimates of upper-crust extension here are considerably underestimated. These extension estimates will also be minimum estimates due to the effects of unknown subseismic resolution faulting and internal deformation. Marrett & Allmendinger (1992) suggest that as much as 25–60 per cent of extension across a region occurs by faulting on small faults below seismic resolution. In this study, we use a mixture of data types with varying degree of resolution. The high-resolution seismic reflection data available in the western Gulf of Corinth (described in Bell *et al.* 2008) approximately underestimates extension due to subseismic resolution faulting by <30 per cent (Wormald 2009), whereas lower resolution seismic reflection data from the central part of the rift is likely missing a larger percentage.

WHOLE-CRUST EXTENSION FROM CRUSTAL THINNING

The Moho depth beneath the Corinth Rift has been determined from wide-angle seismic data and gravity modelling (Tiberi *et al.* 2001; Zelt *et al.* 2005; Sachpazi *et al*. 2007, Fig. 3) and shallows from 42 km in the west (22° E) to <30 km in the east (23°E). The stretched crustal thickness (Fig. 2 and Table 1) is calculated by subtracting depth of top basement (Fig. 1B) from Moho depth (Fig. 3). Crustal thickness beneath the extended onshore southern margin is poorly constrained, due to lack of knowledge of basement depth. Pre-rift crustal thickness (Table 1) is estimated to be the same as the present-day crustal thickness away from the influence of Corinth rifting. Moho depth beneath northern Greece and the Peloponnese follows a similar W to E shallowing trend (resulting from pre-rift crustal thickening of the Hellenide orogeny), with almost N–S striking Moho depth contours (Fig. 3). Locally within the Gulf of Corinth this pattern is distorted due to rifting. In this study the initial crustal thickness for each profile is given by the Moho depth and topography at the point where the Moho contours reach a regional trend, uninfluenced by recent extension (ends of

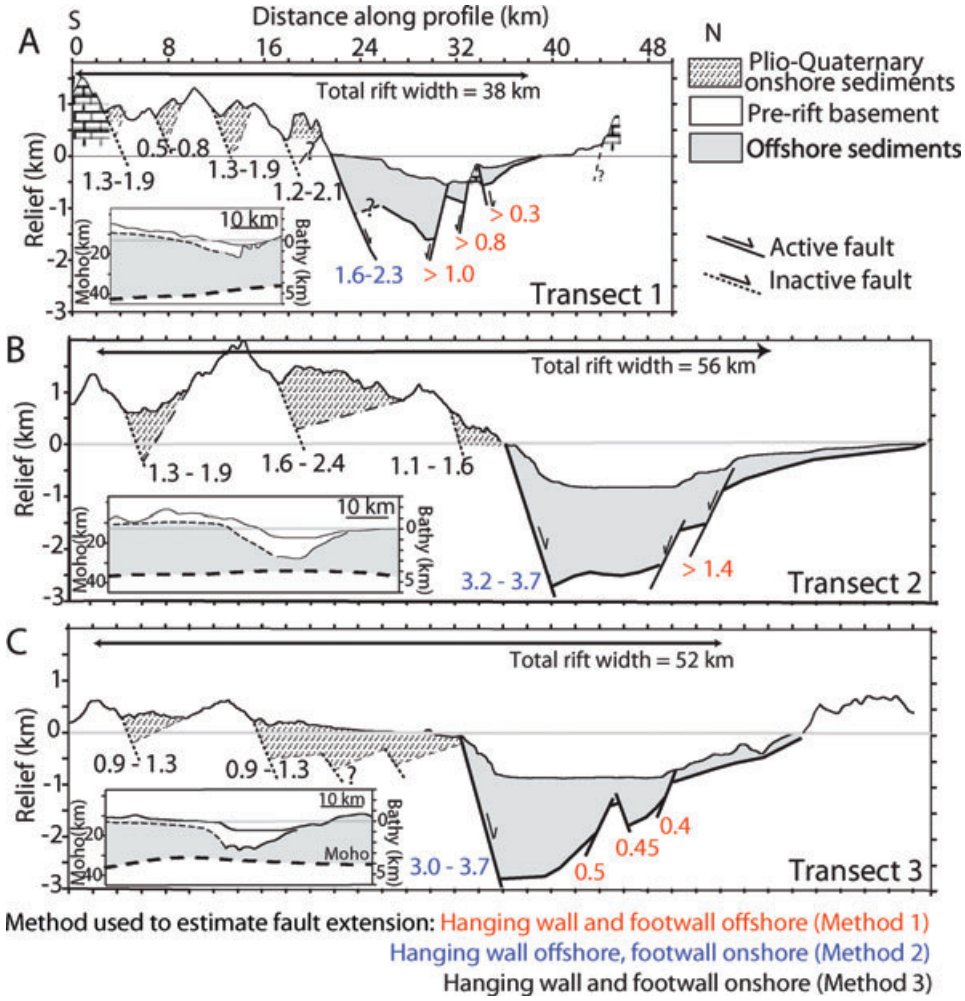

Figure 2. Basement geometry and fault architecture for transects 1–3 following Bell *et al*. (2009). Estimates of fault throw (numbers adjacent to faults, shown in kilometres) are colour coded depending on the method used to determine them (see Supporting Information). Insets in bottom left hand corner of each transect show the sea bed and basement at the scale of the right-hand axis (solid line from Bell *et al.* 2009, dashed lines are unknown basement) and Moho depth at the scale of the left-hand axis (Sachpazi *et al.* 2007).

white lines in Fig. 3). We therefore incorporate the effects of variable pre-rift topography in our estimates of total extension.

Assuming linear variation of stretching across the rift, we derive an average stretching factor (β) for each profile (see the Supporting Information for derivation):

$$\beta = \frac{2i}{i + f}$$

where i and f are the original and maximum stretched crustal thicknesses, respectively (Table 1). The original rift width, and hence total extension, is determined using β and an estimated total stretched rift width, that is, the width of the rift, which has experienced crustal thinning (white lines in Fig. 3, Table 1). Estimating total stretched rift width is complicated for the eastern rift (transects 3) by possible earlier extensional events suggested by some authors, which generated NW–SE trending lobes of shallow Moho beneath the south-east Gulf of Corinth margin (Fig. 1A; Tiberi *et al.* 2001; Zelt *et al.* 2005).

Estimates of total extension based on crustal thinning range from ∼9–13 km in the west along transect 1, and ∼12–21 km in the central Corinth Rift along transects 2 and 3. These estimates are

Table 1. Input parameters used to determine estimates of extension along transects 1–3 in Fig. 2.

	Transect 1	Transect 2	Transect 3
Max. basement depth (km)	1.6	2.8	2.7
Total fault controlled rift width (km)	38	56	52
Total throw from upper-crustal faults (km)	8.0–11.1	8.6–11.0	6.2–7.7
Initial crustal thickness (km)	43–45	39–41	38–40
Minimum crustal thickness of offshore rift derived from Moho depth (km)	36	31	29.5
Minimum crustal thickness of offshore rift derived from basement depth (km)	39	31	30.5
Width of rift which has experienced crustal thinning (see Fig. 1, km)	110–130	140–160	110–160
(A) Total upper-crustal fault extension for 40 – 60° dipping faults (km)	4.6–13.2	4.9–13	3.6–9.2
(B) Whole-crust extension using Moho derived stretched crustal thickness (km)	9–13	14.5–19.5	12–21
(C) Whole-crust extension using basement depth derived crustal thickness (km)	5–8.5	14.5–19.5	11–19

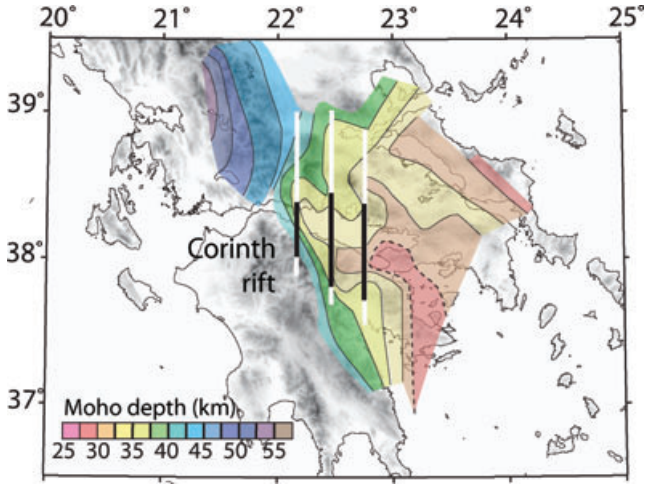

Figure 3. Present-day Moho depth from Sachpazi *et al.* (2007) and locations of transects 1–3. White lines show the estimated width of the Corinth Rift influenced by N–S extension.

subject to errors in estimated initial crustal thickness and total rift width, and effects of previous extensional events.

WHOLE-CRUSTAL EXTENSION FROM BASEMENT SUBSIDENCE

Basement subsidence during extension also provides an estimate of crustal thinning, if Airy isostasy is assumed. The benefits of this method over the crustal thickness method are that pre-rift Moho depth variability that is not related to the current extension episode will not affect the total extension estimate. However, errors in the choice of pre-rift crustal thickness will remain. We determine maximum tectonic subsidence by backstripping the basement surface along each transect, using sediment, crustal and mantle densities of 2000 kg m^{-3}, 2800 kg m^{-3} and 3300 kg m^{-3}, respectively. Assuming Airy isostasy and the initial crustal thickness estimates in Table 1 for the height of the reference column, the tectonic subsidence is then used to determine stretched crustal thickness to derive average β values and then total extension (Table 1).

Using this basement subsidence method we derive a total extension of ∼5–9 km in the west along transect 1, and ∼11–20 km in the central rift along transects 2 and 3.

CORINTH RIFT EXTENSION MECHANISM

Estimates of whole-crust extension determined using the degree of crustal thinning and basement subsidence are generally within error, and indicate greater degrees of whole-crust extension in the central Corinth Rift along transects 2 and 3 (∼11–21 km) than in the west along transect 1 (∼5–13 km, Fig. 4). Upper-crust extension estimates along transects 2 and 3 are lower than estimated whole-crust extension, however as described earlier we suspect a significant contribution of extension from unknown onshore faults in the Akrata to Corinth area and subseismic faulting (e.g. Marrett & Allmendinger 1992). Although our upper-crust extension estimates quantify the majority of extension they are still minimum extension values, which may account for the discrepancy between upper-crust and whole-crust extension values.

In the western Corinth Rift along transect 1, estimates of upper-crust extension (∼5–13 km) are comparable with whole-crust extension derived from both crustal thinning (∼9–13 km) and basement subsidence (∼5–9 km, Fig. 4). Offshore and onshore faulting are best constrained in this part of the rift, and we are confident that all major faults are included (Fig. 2A). The similar upper- and whole-crust extension estimates (Fig. 4) suggest that this part of the rift is undergoing uniform stretching (McKenzie 1978).

A low-angle detachment fault dipping at 5–10° has been proposed beneath the western rift (e.g. Rigo *et al.* 1996; Sorel 2000). Significant low-angle faults would cause upper-crust extension to be underestimated, as they have proportionally larger heave components. We have found no deficit between upper- and whole-crustal extension when using a planar fault assumption, in fact our upper-crustal extension estimate is likely underestimated due to the omission of minor faulting. Low-angle faulting is therefore not necessary to explain long-term deformation in the western Corinth Rift. The total amount of crustal extension across the rift is small (4–13 km) and only one generation of planar faulting is required to produce this degree of extension (Reston 2005).

HOW REPRESENTATIVE ARE MODERN GEODETIC EXTENSION RATES OF LONG-TERM EXTENSION?

GPS data sets indicate that the highest extension rates over the last 5–100 yr occur in the western Corinth Rift at the longitude of Aigion (Fig. 4A). Briole *et al.* 2000's data suggest a rather subtle increase in extension rates from Corinth to Aigion, whereas Clarke *et al*. (1998) present a trend line through their data with a much larger E–W gradient and a continued increase in rates west of Aigion towards the Rion Straits (Fig. 4A). The interpreted short-term extension rate trend presented by Clarke *et al*. (1998) mismatches the longer term 400 kyr fault displacement pattern and long-term rift geometry, which both indicate lower levels of extension west of Aigion than in the centre of the rift (Fig. 4).

Our results show the greatest whole-crust extension during the present phase of rifting is across the central Corinth Rift (transects 2 and 3 at distances of 88 and 117 km along the rift-axis trending profile, respectively, Fig. 4E). The central rift (80–118 km along the rift-axis profile) is also the location of greatest basement subsidence (Fig. 4C), thickest syn-rift infill (Fig. 4D) and apparently greatest rift width (Fig. 1C). Summed Late Quaternary fault displacement is greatest across the central rift, between 67 and 115 km along the rift-axis profile, and decreases to the east and west producing a 'bell-shaped' profile (Fig. 4B). We note that both the maximum geodetic extension rates and greatest summed Late Quaternary fault displacement are offset to the west of the region which has experienced the greatest total extension over rift history.

Clarke *et al*. (1998) have proposed that the strong E–W increase in extension rates interpreted from their data is a long-term feature of extension in the Corinth Rift, and provides evidence for E–W propagation of faulting. Lateral propagation of faulting in the Corinth Rift has previously been challenged by the similarity in the age of the initiation of Corinth Rift active faults in the east and west from onshore (McNeill *et al.* 2005; Leeder *et al*. 2008) and offshore data (Bell *et al.* 2009). In this study we conclude that a strong E–W increasing trend of geodetic extension rates, interpreted by Clarke *et al*. (1998), cannot have persisted over rift history as it is incompatible with the overall rift morphology (Fig. 4). We note here, however, that the strong E–W gradient and increasing extension rate west of Aigion presented by Clarke *et al*. (1998) is largely based on one 1890s triangulation position (TMFR) and two GPS stations (CG30

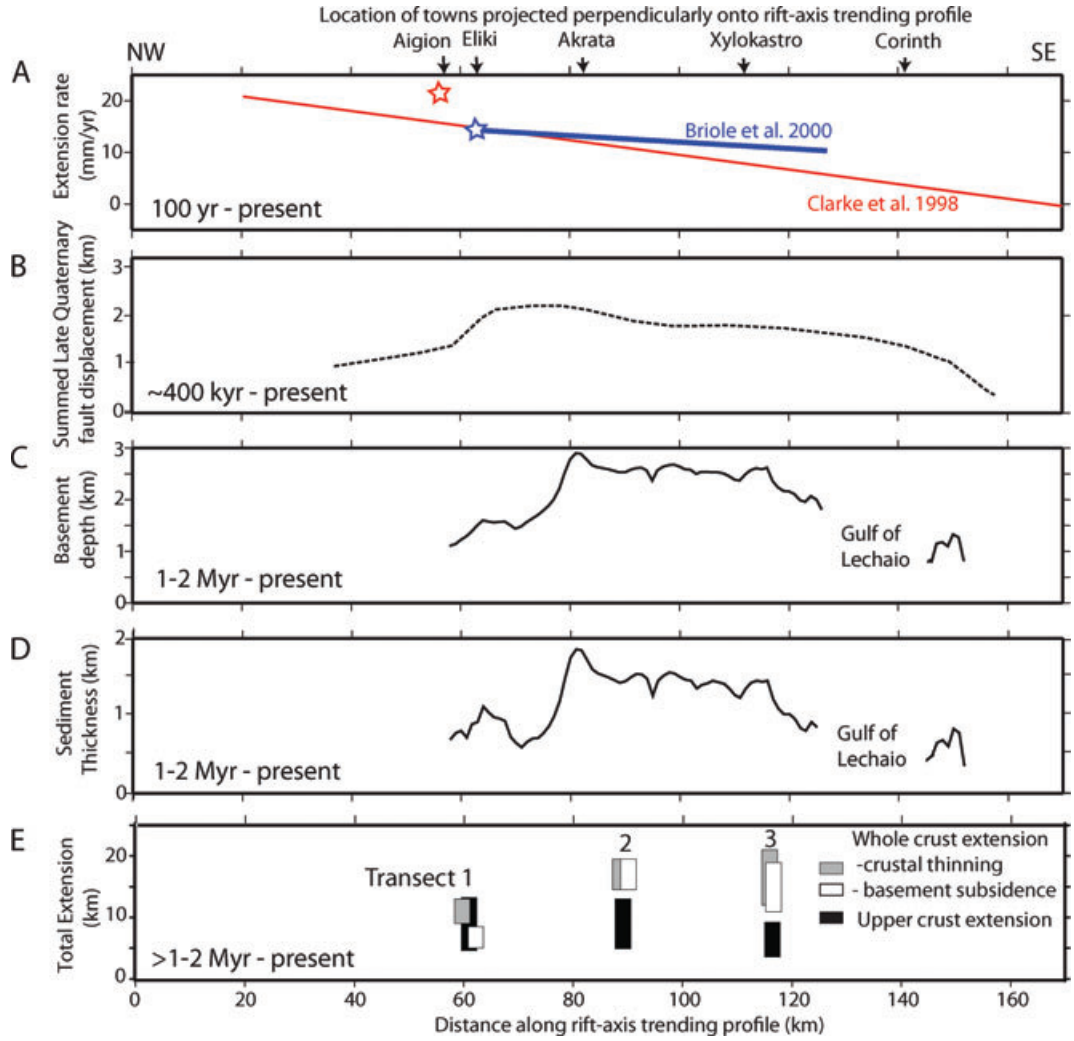

Figure 4. (A) Trend lines through the geodetic data presented by Clarke *et al.* (1998) and Briole *et al.* (2000) and shown in Fig. 1(A). Stars show the location of the greatest extension rate recorded in each study. (B) Late Quaternary fault displacement summed across the rift. (C) Maximum basement depth projected along the red profile shown in Fig. 1(A). Greatest basement depth in the Gulf of Lechaio is unknown. (D) Maximum sediment thickness projected along the red profile shown in Fig. 1(A). Greatest sediment thickness in the Gulf of Lechaio is unknown. (E) Summary of upper-crustal extension derived from faulting along each transect (black bar) and whole-crustal extension derived from crustal thinning (grey bar) and basement subsidence (white bar). Time range over which each figure is providing an assessment of extension distribution is shown in bottom left-hand corner of Figs 4(A)–(E).

and CG31) with anomalous velocity directions (fig. 12 Clarke *et al*. 1998). If these data points are not considered the Clarke *et al*. (1998) and Briole *et al.* (2000) data correlate well and suggest a gradual increase in extension rates to the west, with maximum values in the Aigion area. The Briole *et al.* (2000) pattern of gently increasing extension rates is compatible with the pattern of summed Late Quaternary fault displacement in the central (~80–120 km) part of the rift (Fig. 4).

In summary, the short-term 5- to 100-yr geodetic extension pattern is recording a current focus of extension in the Aigion region (Briole *et al*. 2000), and potentially further west based on the interpretation of Clarke *et al.* (1998). Late Quaternary fault displacement has a bell-shaped profile along the rift with greatest levels of extension focused east of the maximum geodetic extension rates, with the main discrepancy between 60 and 80 km along the rift-axis profile (Fig. 4). Total extension over the 1–2 Myr Corinth Rift history, similarly shows a bell-shaped profile with greatest whole-crust extension, deepest basement depth and thickest sediment deposition occurring in the central rift between 80 and 120 km along the rift-axis trending profile in Fig. 1(C). At some point in the last 400 kyr there appears to have been a shift in the focus of extension from the central rift, to the Aigion–Eliki region further west.

Apparent mismatches between geodetic and geological rates of extension have also been reported in the Apennines (e.g. Papanikolaou *et al.* 2005) and eastern California (Oskin *et al.* 2008). These mismatches have been explained by variations in strain rate over the seismic cycle, only a part of which is sampled geodetically over decadal timescales. In the Corinth Rift, however, we report that both geodetic extension rates and patterns of Late Quaternary fault displacement mismatch the longer term 1–2 Myr rift morphology to some extent.

Temporal changes in fault activity are recorded in the stratigraphy of the Gulf of Corinth (e.g. Bell *et al.* 2009), suggesting relatively rapid changes in spatial strain distribution may be a characteristic feature of rift development. We suggest variations in the locus of maximum extension are associated with fault growth and linkage, as described from outcrop and numerical models (Schlische & Anders 1996; Morley & Wonganan 2000). Fault systems within the Corinth

Rift have evolved to produce an overall simple 'bell-shaped' extension pattern along the rift zone, similar to the idealized displacement profile of individual faults. Similar patterns of rift evolution have been reported from syn-rift geometry in the Lake Malawi basin. Contreras *et al.* (2000) describe how multiple fault systems evolve towards a flattened 'bell-shaped' total displacement profile given enough time to evolve. We suggest the discrepancy between short-term and long-term extension patterns in the Gulf of Corinth do not indicate E–W propagation, but are related to shifts in the loci of maximum extension due to fault growth and linkage. Temporal variations in strain distribution throughout rift history are likely characteristic of rift development in general, and the use of geodetic extension rates as proxies for long-term rift development should be made with caution.

CONCLUSIONS

In the western Corinth Rift, upper- and whole-crust extension estimates agree within error (both ∼5–13 km). We suggest that uniform pure-shear stretching produces the observed rift structure here, without the need for a low-angle detachment mechanism in this area as has previously been suggested.

Total extension over the Corinth Rift's 1–2 Myr history has been greater across the central rift (∼11–21 km), than to the west (∼5–13 km). Summed Late Quaternary fault displacements similarly show a 'bell-shaped' displacement profile with greatest levels of extension focused in the central part of the rift. The highest Late Quaternary fault displacement occurs, however, ∼15 km to the west of the location of deepest rift basement. Short-term 5- to 100-yr geodetic extension rates indicate a current focus of extension in the Aigion region of the Corinth Rift, and potentially further west. The E–W increase in strain rates interpreted from geodetic data cannot have persisted over rift history to produce the simple 'bell-shaped' rift displacement. We suggest the discrepancy between short-term and long-term extension patterns in the Gulf of Corinth do not indicate E–W propagation of faulting, but are related to shifts in the loci of maximum extension due to fault growth and linkage as the Corinth Rift system has evolved.

ACKNOWLEDGMENTS

We thank the crew of the MV Vasilios for their expertise during the western Gulf of Corinth survey. We are grateful to Richard Collier, Carol Cotterill, John Davis, George Ferentinos, Aggeliki Georgiopolou, Alfred Hirn, Mireille Laigle, Mike Leeder, Chris Malzone, George Papatheodorou and Aris Stefatos, for technical and scientific contributions and providing access to other seismic data sets. We also thank the Greek authorities for permission to conduct this work. Research was funded by Natural Environment Research Council grants NER/B/S/2001/00269 and NER/S/A/2004/12634, the University of Southampton, and the Royal Society. We thank reviewers P. Briole, T. Reston and Editor S. Goes for helpful comments, and I. Papanikolaou, A. Pizzi, P. Cowie and an anonymous reviewer for constructive criticism of an earlier version.

REFERENCES

Abers, G.A., 2009. Slip on shallow-dipping normal faults, *Geology,* **37,** 767–768.

Avallone, A. *et al*., 2004. Analysis of eleven years of deformation measured by GPS in the Corinth Rift Laboratory area, *Comptes Rendus Geosciences,* **336,** 301–311.

Bell, R.E., McNeill, L., Bull, J.M. & Henstock, T.J., 2008. Evolution of the offshore western Gulf of Corinth, *Geol. Soc. Am. Bull.,* **120,** 156–178.

Bell, R.E., McNeill, L., Bull, J.M., Henstock, T.J., Collier, R.E.L. & Leeder, M.R., 2009. Fault architecture, basin structure and tectonic evolution of the Corinth rift, central Greece, *Basin Res.,* **21,** 824–855.

Bernard, P. *et al*., 1997. The Ms = 6.2, June 15, 1995 Aigion earthquake (Greece): evidence for low angle normal faulting in the Corinth rift, *J. Seismol.,* **1,** 131–150.

Billiris, H. *et al*., 1991. Geodetic determination of tectonic deformation in central Greece from 1900 to 1988, *Nature,* **350,** 124–129.

Briole, P. *et al*., 2000. Active deformation of the Corinth rift, Greece: results from repeated Global Positioning System surveys between 1990 and 1995, *J. geophys. Res.,* **105,** 25 605–25 625.

Clarke, P.L. *et al*., 1998. Crustal strain in central Greece from repeated GPS measurements in the interval 1989–1997, *Geophys. J. Int.,* **135,** 195–214.

Collier, R. & Jones, G., 2003. Rift sequences of the Southern Margin of the Gulf of Corinth (Greece) as exploration/production analogues, in *AAPG International Conference*, Barcelona, Search and Discovery Article #90017.

Contreras, J., Anders, M.H. & Scholz, C.H., 2000. Growth of a normal fault system: observations from the Lake Malawi basin of the east African rift, *J. Struct. Geol.,* **22,** 159–168.

Dixon, T.H., Norabuena, E. & Hotaling, L., 2003. Paleoseismology and global positioning system: earthquake-cycle effects and geodetic versus geologic fault slip rates in the Eastern California shear zone, *Geology,* **31,** 55–58.

Floyd, M.A. *et al*., 2010. A new velocity field for Greece: implications for the kinematics and dynamics of the Aegean, *J. geophys. Res.,* **115,** B10403, doi:10.1029/2009JB007040.

Ford, M., Williams, E.A., Malatre, F. & Popescu, S.P., 2007. Stratigraphic architecture, sedimentology and structure of the Vouraikos Gilbert–type delta, Gulf of Corinth, Greece, in *Sedimentary Processes, Environments and Basins,* Int. Assoc. Sediment. Spec. Pub. 38, pp. 49–90, eds Paola, C., Nichols, G.J., Williams, E.A., Wiley-Blackwell, Chichester.

Hatzfeld, D., Karakostas, V., Ziazia, M., Kassaras, I., Papadimitriou, E., Makropoulos, K., Voulgaris, N. & Papaioannou, 2000. Microseismicity and faulting geometry in the Gulf of Corinth (Greece), *Geophys. J. Int.,* **141,** 438–456, doi:10.1046/j.1365-246x.2000.00092.x.

Kusznir, N.J., Hunsdale, R., Roberts, A.M. & Team, I., 2005. Norwegian margin depth-dependent stretching, in *Petroleum Geology: North-West Europe and Global Perspectives, Proceedings of the 6th Petroleum Geology Conference*, eds Dore, A.G. & Vining, B.A., Geological Society, London.

Lamarche, G., Barnes, P.M. & Bull, J.M., 2006. Faulting and extension rate over the last 20,000 years in the offshore Whakatane Graben, New Zealand continental shelf, *Tectonics,* **25**, doi:10.1029/2005TC001886.

Leeder, M., Seger, M.J. & Stark, C.P., 1991. Sedimentation and tectonic geomorphology adjacent to major active and inactive normal faults, southern Greece, *J. Geol. Soc., Lond.,* **148,** 331–343.

Leeder, M.R., Mack, G.H., Brasier, A.T., Parrish, R., Mcintosh, W.C., Andrews, J.E. & Duermeijer, C.E., 2008. Late-Pliocene timing of Corinth (Greece) rift-margin fault migration, *Earth planet. Sci. Lett.,* **274,** 132–141.

Marrett, R. & Allmendinger, R.W., 1992. Amount of extension on "small" faults: an example from the Viking graben, *Geology,* **20,** 47–50.

Mckenzie, D.P., 1978. Some remarks on the development of sedimentary basins, *Earth planet. Sci. Lett.,* **40,** 25–32.

McNeill, L.C., Collier, R.E.L., De Martini, P., Pantosti, D. & D'Addezio, G., 2005. Recent history of the Eastern Eliki Fault, Gulf of Corinth: geomorphology, palaeoseismology and impact on palaeoenvironments, *Geophys. J. Int.,* **161,** 154–166.

Morley, C.K. & Wonganan, N., 2000. Normal fault displacement characteristics, with particular reference to synthetic transfer zones, Mae Moh mine, northern Thailand, *Basin Res.,* **12,** 307–327.

Oskin, M., Perg, L., Shelef, E., Strane, M., Gurney, E., Singer, B. & Zhang, X., 2008. Elevated shear zone loading rate during an earthquake cluster in eastern California, *Geology,* **36,** 507–510.

Papanikolaou, I.D., Roberts, G.P. & Michetti, A.M., 2005. Fault scarps and deformation rates in Lazio-Abruzzo, Central Italy: comparison between geological fault slip-rate and GPS data, *Tectonophysics,* **408**, 147–176.

Reston, T.J., 2005. Polyphase faulting during the development of the West Galicia rifted margin, *Earth planet. Sci. Lett.,* **237,** 561–576.

Reston, T., 2007. Extension discrepancy at North Atlantic nonvolcanic rifted margins: depth-dependent stretching or unrecognized faulting? *Geology,* **35,** 367–370.

Rigo, A., Lyon-Caen, H., Armijo, R., Deschamps, A., Hatzfeld, D., Makropoulos, K., Papadimitriou, P. & Kassaras, I., 1996. A microseismic study in the western part of the Gulf of Corinth (Greece): implications for large-scale normal faulting mechanisms, *Geophys. J. Int.,* **126**, 663–688.

Roberts, G.P., 1996. Variation in fault-slip direction along active and segmented normal fault systems, *J. Struct. Geol.,* **18,** 835–845.

Rohais, S., Eschard, R., Ford, M., Guillocheau, F. & Moretti, I., 2007. Stratigraphic architecture of the Plio-Pleistocene infill of the Corinth Rift: implications for its structural evolution, *Tectonophysics,* **440,** 5–28.

Sachpazi, M. *et al*., 2007. Moho topography under central Greece and its compensation by Pn time-terms for the accurate location of hypocenters: the example of the Gulf of Corinth 1995 Aigion earthquake, *Tectonophysics,* **440,** 53–65.

Schlische, R.W. & Anders, M.H., 1996. Stratigraphic effects and tectonic implications of the growth of normal faults and extensional basins, *Geol. Soc. Am. Spec. Publ.,* **303,** 183–203.

Skourlis, K. & Doutsos, T., 2003. The Pindos Fold-and-thrust belt (Greece): inversion kinematics of a passive continental margin, *Int. J. Earth Sci.,* **92,** 891–903.

Sorel, D., 2000. A Pleistocene and still-active detachment fault and the origin of the Corinth-Patras rift, Greece, *Geology,* **28,** 83–86.

Tiberi, C., Diament, M., Lyon-Caen, H. & King, T., 2001. Moho topography beneath the Corinth Rift area (Greece) from inversion of gravity data, *Geophys. J. Int.,* **145,** 797–808.

Wallace, L.M., Ellis, S., Miyao, K., Miura, S., Beavan, J. & Goto, J., 2009. Enigmatic, highly active left-lateral shear zone in southwest Japan explained by aseismic ridge collision, *Geology,* **37,** 143–146.

White, N., 1990. Does the uniform stretching model work in the North Sea?, in *Tectonic Evolution of the North Sea Rifts*, eds Blundell, D.J. & Gibbs, A.D., Oxford University Press, Oxford.

Wormald, S.C., 2009. Strain and strain rates in the offshore Gulf of Corinth. *M.Geophys*. Thesis, University of Southampton.

Zelt, B.C., Taylor, B., Sachpazi, M. & Hirn, A., 2005. Custal velocity and Moho structure beneath the gulf of Corinth, Greece, *Geophys. J. Int.,* **162,** 257–268.

SUPPORTING INFORMATION

Additional Supporting Information may be found in the online version of this article:

Supplement. This supplementary material contains a figure (Fig. S1) and figure caption fully labelling major active and inactive faults within the Corinth Rift. It also contains an explanation of the methods used to derive fault throw in this study for onshore, offshore and partially offshore and onshore faults. In addition, we present a derivation of the average β factor as used in this study.

Please note: Wiley-Blackwell are not responsible for the content or functionality of any supporting materials supplied by the authors. Any queries (other than missing material) should be directed to the corresponding author for the article.